ISBN: 978-3-95450-222-6 ISSN: 2673-5350 doi:10.18429/JACoW-IBIC2020-TUPP35

DEVELOPMENT OF A THERMAL RESPONSE MODEL FOR WIRE GRID PROFILE MONITORS AND BENCHMARKING TO CERN LINAC4 EXPERIMENTS

A. Navarro*, F. Roncarolo, CERN, Geneva, Switzerland
M. Sapinski, TERA Fundation

Abstract

The operation of wire grids as beam profile monitors, both in terms of measurement accuracy and wire integrity, can be heavily affected by the thermal response of the wires to the energy deposited by the charged particles. A comprehensive model to describe such interaction has been implemented including beam induced heating, all relevant cooling processes and the various phenomena contributing to the wire signal such as secondary emission and H^- electron scattering. The output from this model gives a prediction of the wire signal and temperature evolution under different beam conditions. The model has been applied to the wire grids of the CERN LINAC4 160 MeV H^- beam and compared to experimental measurements. This successful benchmarking allowed the model to be used to review the beam power limits for operating wire grids in LINAC4.

INTRODUCTION

Wire Grid Profile monitors [1] are extensively used for transverse beam profile measurements in linacs and transfer lines. They consist of a series of thin wires supported on a frame, as shown in Fig. 1. The signal on each wire, used to reconstruct the beam profile, is generated by a combination of different phenomena occurring after the beam-wire interaction, such as direct charge deposition (e.g. stripped electrons stopped in the wire in the case of H^- beams), secondary emission of electrons, thermionic emission of electrons, etc. In most cases these wire grids are movable devices that are inserted into the beam line only when needed.

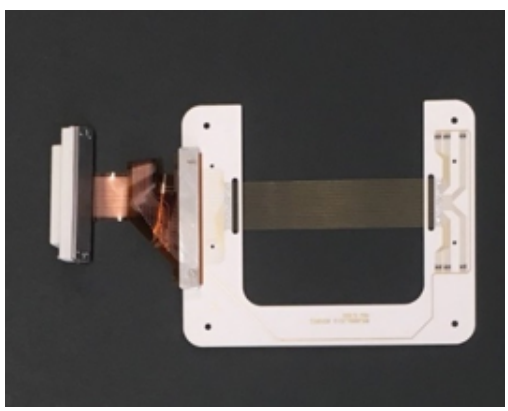

Figure 1: Example of a Wire Grid recently installed in the CERN LINAC4, featuring 40 µm tungsten wires separated by 0.5 mm.

* araceli.navarro.fernandez@cern.ch

For a given wire grid detector design and materials, the beam power density, defined by beam intensity, transverse size and longitudinal structure, can generate high wire temperatures, which may perturb the measurement accuracy or even damage the detector. An example of such an issue is shown in Fig. 2, where a LINAC4 grid suffered overheating of the wires after operation at 160 MeV. This prompted the need for a thorough understanding of the wire temperature evolution in order to correctly retrieve the transverse beam characteristics and set operational limits on the beam power allowed for grid use.

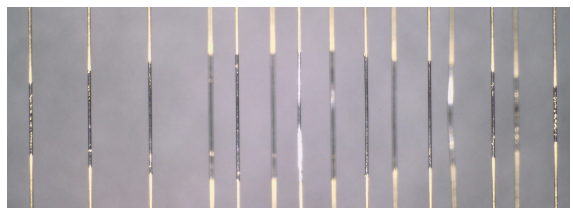

Figure 2: Effect of wire gird heating as observed with an optical microscope, with the individual wires visible over the grey background. The evaporation of the gold coating (dark central area on each wire) is clearly visible, from which one can even infer the beam density profile in the plane of measurement.

The original LINAC4 wire grid design was already supported by theoretical calculations of the thermal response [2, 3]. However, the operational limits defined by this approach clearly did not take into account all phenomena. We therefore adopted and applied another model, initially developed for fast wire scanners [4], with the aim of bench-marking dedicated beam measurements and defining operational limits.

Measuring the temperature evolution of thin wires as they interact with particle beams is challenging. Firstly, the temperature range is broad, from 300 K up to 3000 K, which excludes the use of contact thermometers [5]. Secondly, the small wire diameters makes the use of optical methods [6] very difficult. Bench-marking of the simulations is therefore based on the observation of thermionic currents, occurring at well know temperatures, similar to the studies presented in [7] for measuring stripping foil temperatures.

HEATING MODEL

During operation, the wire temperature increase due to particles energy deposition is accompanied by various cooling processes occurring both during and after the beam passage.

ISBN: 978-3-95450-222-6 ISSN: 2673-5350 doi:10.18429/JACoW-IBIC2020-TUPP35

These include radiative, conductive, thermionic and sublimation cooling. The instantaneous temperature variation during a beam pulse can be written as:

$$\Delta T_{Tot} = \Delta T_{Ht} - \Delta T_{Rd} - \Delta T_{Con} - \Delta T_{Th} - \Delta T_{Sub} \quad (1)$$

Each term of this equation will be discussed in the following subsections.

Wire Heating

The temperature increase generated by N_i particles in a detector volume ΔV can be expressed as:

$$\Delta T_{Ht} = \frac{N_i}{\Delta V \cdot Cp(T) \cdot \rho} \cdot \frac{dE}{dx} \quad (2)$$

where dE/dx is the single particle energy deposition normally well described by the Bethe-Bloch formula [8], and simulated with GEANT4 [9] for these studies. ρ the wire material density and C_p the specific heat capacity (temperature dependent).

Radiative Cooling

Black body radiation, usually the dominant cooling effect in a vacuum, is described by the Stephan-Boltzmann law:

$$\Delta T_{rd} = \frac{\Delta S \cdot \sigma_{SB} \cdot \epsilon(T) \cdot (T^4 - T_0^4)}{C_p(T) \cdot \Delta V \cdot \rho} \cdot \Delta t \quad (3)$$

where σ_{SB} is Stephan-Boltzmann constant , ϵ the emissivity of the material (temperature dependent) and ΔS is the surface of the volume ΔV which radiates during the time Δt.

Thermionic Cooling

Thermionic electron emission occurs when the energy transferred to the electrons by thermal excitation exceeds their work function. The electron emission contributes both to the signal on the wire and to the cooling. The Richardson-Dushman equation describes the current density, J_{Th}, generated in the wire due to thermionic emission:

$$J_{Th} = A_R \cdot T^2 \cdot exp\left(-\frac{\phi}{k_B T}\right) \quad (4)$$

where ϕ is the work function of the material, A_R the Richardson constant and k_b Bolzmann's constant. The resulting cooling contribution, ΔT_{Th} can be written as:

$$\Delta T_{Th} = \Delta S \cdot (\phi + 2\sigma_B T) \cdot \frac{J_{Th}}{C_p(T) \cdot \Delta V \cdot \rho} \cdot \Delta t \quad (5)$$

Conductive Cooling

Thermal conduction is the transfer of heat within a body. The one dimensional heat equation is described as

$$\frac{\partial T}{\partial t} = \alpha(T)\frac{\partial^2 T}{\partial x} \qquad 0 \le x \le L \qquad t \ge 0 \quad (6)$$

where α(T) is related to the thermal conductivity by $\alpha(T) = \lambda(T)/\rho C_p(T)$. In our model, this equation is integrated over the wire length L, with the boundary condition $T(0,t) = T(L,t)$ =300 K.The numerical solution is implemented via a Forward Time Centered Space (FTCS) approximation [10].

Sublimation Cooling

At high temperatures, another cooling term can appear due to energy transfer during the material sublimation process. Without considering the variation in the wire diameter and thus the change in mass and heat capacity, the temperature variation due to sublimation can be written as:

$$\Delta T_{Sub} = -H_{sub} \cdot W(T) \quad (7)$$

where H_{sub} is the enthalpy of sublimation and W(T) the material sublimation rate [11].

INTENSITY MODEL

In addition to the signal generated by thermionic emission according to Eq. (4), which can be significant at high temperatures, each charged particle deposited in the wire also generates a net charge. The electric charge per incident particle ($Q\left(\frac{e}{Proj}\right)$) can be simplified as:

$$Q\left(\frac{e}{Proj}\right) = Q_{dep} + Q_{SE} \quad (8)$$

with Q_{dep} the direct charge deposition and Q_{SE} the contribution from secondary electrons emission.

Charge Deposition

In the general case of accelerated ions with N_p the number of protons in the nucleus and N_e the number of electrons hitting the wire the deposited charge can be estimated as:

$$Q_{dep} = N_p \cdot (1 - BS_p) \cdot (1 - \eta) - N_e \cdot (1 - BS_e) \cdot \mu \quad (9)$$

where BS_p and BS_e refer to the proportion of back-scattered protons and electrons respectively, η the proportion of protons that traverse the wire and μ the proportion of incident electrons that are stopped. For our model, all these parameters were calculated using GEANT4.

Charge due to Secondary Emission

Each charged particle entering or exiting the detector surface has a certain probability of generating secondary electrons (SE) that escape the wire. The model adopted can be summarized as follows:

$$Q_{SE} = N_p \cdot (SEY_{p1} + \eta \cdot SEY_{p2}) \quad (10)$$
$$+N_e \cdot (SEY_{e1} + SEY_{e2} \cdot (1 - \mu)) +$$
$$N_p \cdot BS_p \cdot SEY_{BS_{p1}} + N_e \cdot BS_e \cdot SEY_{BS_{e1}} + Y_D$$

The Secondary Emission Yield (SEY) gives the average number of electrons emitted per incident particle [12]. SEY_p refers to SE generated due to incident protons, while SEY_e refers to SE generated due to incident electrons. The sub indices 1 and 2 represent the wire surfaces, 1 being the first surface encountered by the beam particles and 2 the exiting surface. Y_D is the proportion of SE generated by these secondary electrons themselves and SEY_{BS} accounts for the SE generated by back-scattered particles.

ISBN: 978-3-95450-222-6 ISSN: 2673-5350 doi:10.18429/JACoW-IBIC2020-TUPP35

BENCH MARKING METHOD

Bench-marking of the model is based on the comparison between the wire signals and the beam current measurement from dedicated beam current transformers, for LINAC4 pulses of variable length. The measurements presented here were performed with one of the wire grids located in the 160 MeV LINAC4 section and consisted of 32 wire of 40 µm diameter, made of Tungsten coated with Gold. The main beam parameters are summarized in Table 1.

Table 1: Measured Beam Parameters at the Wire Grid Location, Used as Input for the Simulations

Parameter	Value
Particle	H^- ($N_p = 1$, $N_e = 2$)
Energy	160 MeV
Repetition Rate	0.83 Hz
Beam Position	X_0 = -2.69 Y_0 = −2.64 mm
Beam Size	σ_x = 0.31 σ_y = 2.64 mm

Under the assumption that the beam position and size do not significantly change during the pulse, something verified for the measurements used for the bench-marking, the signal on each wire is proportional to the beam current until the wire temperature increase is high enough (about 2000 K) to make Thermionic emission (Eq. (4)) significant.

The experiment consisted of increasing the beam pulse length in a controlled way in order to gradually reach a beam power on the wires that made thermionic emission evident. This would allow bench-marking of the the model under such a scenario, and use it to predict the wire temperature.

RESULTS AND DISCUSSION

An example of some measurement results is shown in Fig. 3. This shows the signal from a single wire intercepting the beam core over 3 consecutive LINAC4 pulses of 450 µs duration. This signal is compared to the beam current evolution measured by a Beam Current Transformer, which gave similar results for all 3 pulses. The data has been scaled to allow a direct comparison between the two instruments. The intensity modulation during the pulse and the pulse interruptions reflect the real beam properties during these measurements, arising from the source and chopper settings respectively. The plot shows two main characteristics of the wire signal that are fundamental for bench-marking the model:

1. During a pulse the wire heats up due to Thermionic emission, as seen by the divergence of the signal with respect to the intensity measured by the BCT. This effect increases slightly pulse after pulse due to the higher initial wire temperature.
2. In the 1.2 s periods between pulses the wire cools down with thermionic electrons still emitted while the wire is hot directly after the pulse leading to a slightly positive signal.

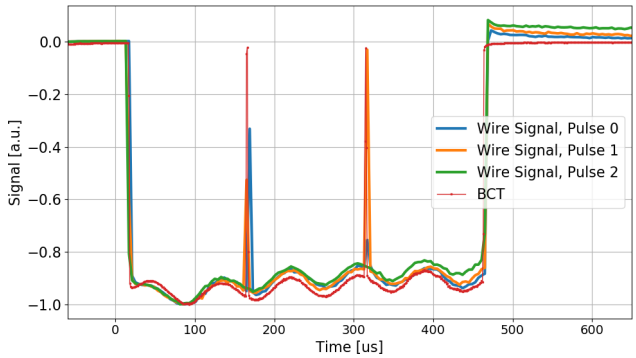

Figure 3: Signal as measured on the wire intercepting the beam core over 3 consecutive LINAC4 pulses of 450 µs duration scaled for comparison with the beam current signal as measured by a beam current transformer.

The wire signal and BCT signals (with the chopper 'holes' removed to make the results clearer) are shown again in Fig. 4, this time together with the output from the model.

The simulation does not currently include a variable beam intensity during the pulse, which is why the modulation caused by the source is not visible. Despite this, the example shows how the model successfully reproduces both of the experimental features described above, namely the divergence from the BCT signal during the pulse and the continued emission of thermionic electrons after the beam passage.

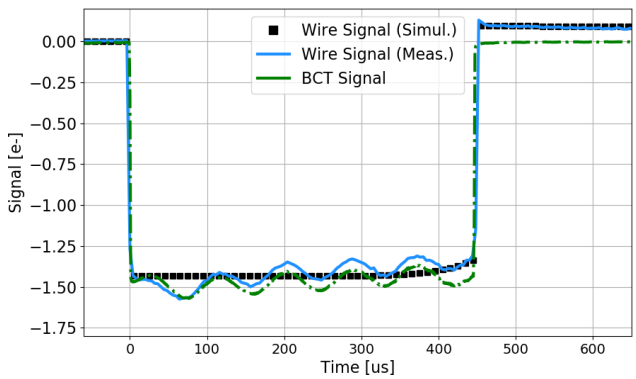

Figure 4: Signal generated in the wire intercepting the beam core as a function of time. Simulated data in black, experimental data in blue.

The agreement between the model and experiment in terms of wire signal versus beam current evolution, is well within 10 % after averaging for the LINAC4 source intensity modulations. Although more experiments and simulation tuning will be needed to fully validate the model, this first result at LINAC4 gives a high degree of confidence that such a model can be used to accurately simulate wire temperatures. Figure 5 shows the simulated maximum temperature reached by the wire during 6 consecutive LINAC4 pulses. A very fast temperature increase can be observed during the beam passage, followed by a comparatively slow cooling. The repetition rate of the beam is currently low enough for the maximum temperature to stabilize after six pulses, to

ISBN: 978-3-95450-222-6 ISSN: 2673-5350 doi:10.18429/JACoW-IBIC2020-TUPP35

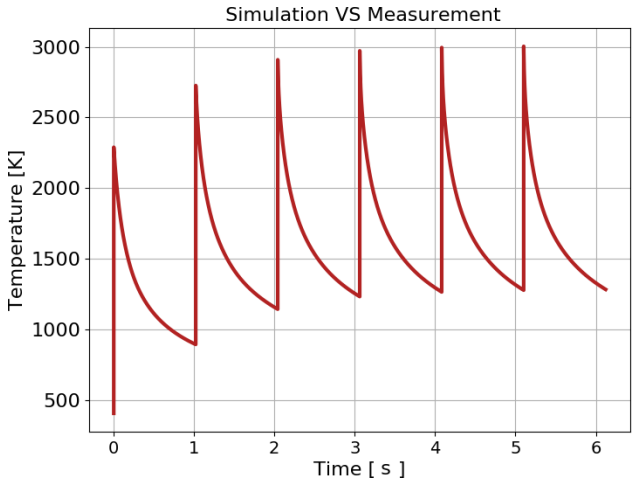

Figure 5: Maximum wire temperature as inferred from the simulation of the bench-marking experiment

about $T_{max} = 3000$ K. This is compatible with the observed evaporation of the wire gold coating without damage to the tungsten core, as confirmed by the visual inspection of the grid after the experiment.

SIMULATION OF LINAC4 BEAM POWER LIMITS FOR GRIDS OPERATION AT 160 MeV

The model can be applied to a variety of beam parameters and wire characteristics, and has allowed a re-calculation the LINAC4 beam power limits at 160 MeV to minimize the risk of overheating and damaging the tungsten wires. This results in plots like the one in Fig. 6 for all wire grids that maintains the maximum temperature reached below 1400 K (the limit for gold coating evaporation), for a variety of beam characteristics in terms of pulse length and total current.

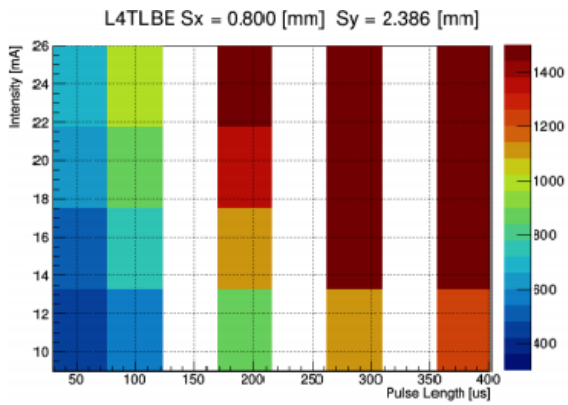

Figure 6: Maximum temperature reached by wire grid detectors for several intensity and pulse length combinations.

OUTLOOK

A first version of a comprehensive model simulating wire grid electrical signal generation and thermal evolution induced by intense ion beams has been bench-marked with beam based experiments using the LINAC4 H^- beam at 160 MeV. The model has been proven to reproduce well the onset of thermionic emission, which can then be used as an indirect wire temperature measurement. The results obtained give a high degree of confidence in the simulation of the beam power limits for the safe operation of the high energy wire grids in LINAC4. As a continuation of this work, the model will be applied to other wire grids and beams in the CERN complex, as well as to fast wire scanners.

In parallel, it is planned to experimentally enhance the accurate determination of some key input parameters, such as the material surface emissivity, that for the moment are only inferred from literature.

REFERENCES

[1] U.Raich, "Beam Diagnostics", Geneva, CERN, pp. 503-514, 2014. https://cds.cern.ch/record/1693047/files/p503.pdf

[2] B. Cheymol, "Development of beam transverse profile and emittance monitors for the CERN LINAC4", Geneve, LPC, 2011. http://cds.cern.ch/record/1503551

[3] F. Zocca *et al.*, "Profile and Emittance Measurements at the CERN LINAC4 3MeV Test Stand", in *Proc. IBIC'13*, Oxford, UK, paper WEPF09, pp. 826-829, 2013.

[4] M. Sapinski, "Model of Carbon Wire Heating in Accelerator Beam", Geneva, CERN, 2008. https://cds.cern.ch/record/1123363

[5] A. J. Onnink *et al.*, "How hot is the wire: Optical, electrical, and combined methods to determine filament temperature", *Thin Solid Films*, vol. 674, pp. 22-32, 2019. doi:10.1016/j.tsf.2019.02.003

[6] P. Antunes *et al.*, "Thin bonding wire temperature measurement using optical fiber sensors', *Measurement*, vol. 44, no. 3, pp. 554-558, March 2011. doi:10.1016/j.measurement.2010.11.016

[7] T. Spickermann *et al.*, "Stripper Foil Temperatures and Electron Emission at the Los Alamos Proton Storage Ring", in *Proc. PAC'03*, Portland, OR, USA, paper FPAB083, pp. 3455–3457, 2003.

[8] K. Nakamura *et al.*, "Passage of particles through matter", Particle Data Group, JP G37, 075021 (2010) and 2011 partial update for the 2012 edition, pp. 1–42, Feb. 2012. https://pdg.lbl.gov/2011/reviews/rpp2011-rev-passage-particles-matter.pdf

[9] GEANT4, https://geant4.web.cern.ch/

[10] G. W. Recktenwald, "Finite-Difference Approximations to the Heat Equation", *Mechanical Engineering*, vol. 10, pp. 1–27, 2004.

[11] S. Dushman, *Scientific Foundations of Vacuum Technique*, John Wiley & Sons, Inc., New York, 1962 (second edition).

[12] J. Allison *et al.*, "Recent developments in GEANT4", *Nucl. Instrum. Methods Phys. Res., Sect. A*, vol. 835, pp. 186-225, 2016. doi:10.1016/j.nima.2016.06.125